Studia UBB Geologia, 2013, **58** (2), 29 – 40

Sedimentary deposition of Bozeş Formation (Apuseni Mts., Romania) – detrital zircon dating and micropaleontological ages

Ramona BĂLC[1*] & Luminița ZAHARIA[2]

[1]Babeş-Bolyai University, Faculty of Environmental Science and Engineering, Fântânele 30, 400294 Cluj-Napoca, Romania
[2]Babeş-Bolyai University, Museum of Mineralogy and Department of Geology, Kogălniceanu 1, 400084 Cluj-Napoca, Romania

Received: November 2013; accepted January 2014
Available online 17 January 2014
DOI: http://dx.doi.org/10.5038/1937-8602.58.2.4

Abstract. In order to establish the age of the Bozeş Formation, which crops out in the SE Apuseni Mts., calcareous nannofossils investigations and U-Pb detrital zircon dating were performed in the Stăuinii Valley section. The results were correlated, and further compared with previous fossil age data. The U-Pb detrital zircon age spectrum reveals a consistent Late Cretaceous grain population, which yielded an age of 83 Ma (concordia age of 82.87±0.59 Ma), interpreted as the maximum deposition age, thus, marking the Early Campanian as the initiation of sediment deposition. Based on the presence of some important taxa in the calcareous nannofossil assemblage, the age of studied section was assigned to Late Santonian? – late Late Campanian. The Late Santonian age is presumed by the presence of curved *Lucianorhabdus cauyeuxii*, reworked from older deposits. The Campanian stage is confirmed by the presence of *Broinsonia parca parca, Broinsonia parca constricta* and rare specimens of *Ceratolithoides aculeus* and *Uniplanarius sissinghii*. Both *Reinhardtites anthophorus* and *Eiffelithus eximius* indicate that the upper part of the Stăuinii section is ending in CC22 / $UC15_d^{TP}$ – $UC15_e^{TP}$ Subzones, thus in late Late Campanian. First occurrence (FO) of *Eiffellithus parallelus* points to the same age. The calcareous nannofossil assemblages do not sustain the presence of the Lower Maastrichtian deposits in the Stăuinii Valley, as mentioned by few previous studies based on *Pachydiscus neubergicus*.

Keywords: calcareous nannofossils, Campanian, bioevent, marker species, siliciclastic rocks

INTRODUCTION

Sedimentary rocks record data about the composition of continental crust, the changes of climate, the variation of the atmosphere and hydrosphere compositions, as well as the evolution of life during Earth History (Rasmussen, 2005 and references therein). Dating a sedimentary rock means mainly constraining its age in terms of sediment deposition and, in some cases, of the subsequent processes such as diagenesis. In most situations, if present, fossils, i.e. the remains of past organisms provide the easiest way to establish the depositional age of sediments. However, there are cases when sedimentary successions are missing a proper fossil record, or the low abundances or diversity are not suitable for stratigraphic correlation. Alternatively, some indirect, radiometric techniques are also widely involved, as dating contemporaneous volcanic rocks or detrital minerals within the sediment. These, too, cannot be always applied, as many basins lack volcanic rocks, while detrital minerals yields only maximum ages, thus the ages when they formed in their originally magmatic rocks.

The Upper Cretaceous Bozeş Formation from the Apuseni Mountains is widely considered as Santonian - Early Maastrichtian in age, as constrained by several macro- and microfauna-based studies (Macovei and Atanasiu, 1934; Dimian and Popa-Dimian, 1964; Tomescu et al., 1969; Marincaş and Mânecan, 1971; Marincaş, 1973). However, different studies performed even on the same section resulted in different age limits. Placed in the eastern part of Bozeş Formation, the Stăuinii Valley section is such a controversial area regarding the depositional age of sediments, the limits varying from Late Santonian to Early Maastrichtian, depending on the described fossil assemblages and different authors.

For the first time in case of the Bozeş Formation, a radiometric method is used, as U-Pb dating of detrital zircon, and combined with a new complementary calcareous nannofossils study, in order to correlate the results and to constrain better the age of sediment deposition.

GEOLOGICAL SETTING

Although the Apuseni Mountains represent an isolated unit between the Pannonian and the Transylvanian basins, tectonically, they are part of the Alpine-Carpathians mountain belt, being the result of complex plate movements during Mesozoic to Cenozoic. Specifically, the Apuseni Mts. resulted from the collision of the Tisia and Dacia microplates during Cretaceous times (Csontos, 1995), the suture between these two being preserved in the south and southeastern part of the mountains. Several tectonic units are building up the Apuseni Mts., namely Bihor Unit, Apusenides and Western Transylvanides. These units are separated and sub-divided according to the age of the tectonic phases and their corresponding nappe emplacement (Ianovici et al., 1976; Săndulescu, 1984; Balintoni, 1997). In the southern Apuseni Mts, only units belonging to Transylvanides and Apusenides occur (Fig. 1a).

*Correspondence: ramona.balc@ubbcluj.ro

Cropping out in the southeastern part of the Apuseni Mts. (Fig. 1a), the Bozeş Formation represents the uppermost unit among the Western Transylvanides (Ghiţulescu and Socolescu, 1941; Bleahu et al., 1981), although much recently, the Bozeş Formation was tectonically affiliated to Southern Carpathians (Balintoni, 2003), both ideas being in use. The Bozeş Formation consists of *ca.* 3000m-thick, turbidite-type sediments as grey sandstones and silty marls, with fine-grained conglomeratic levels in the upper part (Dimian and Popa-Dimian, 1964). Based on macro- and microfauna, the age of the formation was considered Santonian – Campanian – Early Maastrichtian (Macovei and Atanasiu, 1934; Dimian and Popa-Dimian, 1964; Tomescu et al., 1969; Marincaş and Mânecan, 1971; Marincaş, 1973; Bălc et al., 2007, 2012).

PREVIOUS MICROPALEONTOLOGICAL AGE DATA ON STĂUINII VALLEY

At the beginning of the 20th century, Bozeş sedimentary rocks cropping out in the Stăuinii Valley section were considered by Palfy (1903, in Dimian and Popa-Dimian, 1964) as Campanian in age, due to a macrofauna occurring on various levels, with *Inoceramus*, *Actaeonella*, *Cerithium* and *Sabal major*. Nopcsa (1905, in Macovei and Atanasiu, 1943) reported the presence of *Pachydiscus neubergicus* and *P. colligatus*, based on which Macovei and Atanasiu (1934) assigned an Early Maastrichtian age for parts of the Stăuinii Valley deposits. As a result of a more detailed study on foraminifera assemblages performed along the valley, Dimian and Popa-Dimian (1964) assigned a Late Santonian - Campanian age for the sediments, the base of the section being represented by the upstream deposits, while downwards they become stratigraphically younger. The same authors also described an ammonite fauna, including *P. colligatus* but without *P. neubergicus*. Tomescu et al. (1969) reported a diverse fauna in Stăuinii Valley, including inoceramids and ammonites, *e.g. Inoceramus balticus*, *I. regularis*, *Hoplitoplacenticeras vari*, *Pachydiscus neubergicus* and *P. colligatus*, all occurring at the same level. The authors mentioned the above-described fauna as being specific for the Late Campanian of Western Europe, but with *P. neubergicus* cited from Lower Maastrichtian deposits too. Thus, the Stăuinii deposits were considered by the previous authors as Campanian-Early Maastrichtian in age.

CALCAREOUS NANNOFOSSIL ANALYSES

Due to their abundance, rapid evolution and cosmopolitan character, calcareous nannofossils represent a useful tool in biostratigraphical studies. They are widely used since the 1950s, and all the data obtained were involved in building the biostratigraphic zonation schemes covering the range of calcareous nannofossils (Martini, 1971; Sissingh, 1977; Perch-Nielsen, 1985; Okada and Bukry, 1980; Bown et al., 1998; Burnett, 1998).

Materials and methods

A number of 200 clay samples has been collected from Stăuinii Valley in order to establish the age of the deposits based on calcareous nannofossil assemblages. The smear slides have been processed using the standard method (Bown and Young, 1998). For calcareous nannofossils analyses at least 300 specimens have been identified in each sample and another 1000 FOV (fields of view) have been browsed in order to identify the rare specimens using a Zeiss Axiolab A microscope at 1000x magnification. The pictures of calcareous nannofossils have been captured with an AxioCamERc5s digital camera (Fig. 2). All the identified species

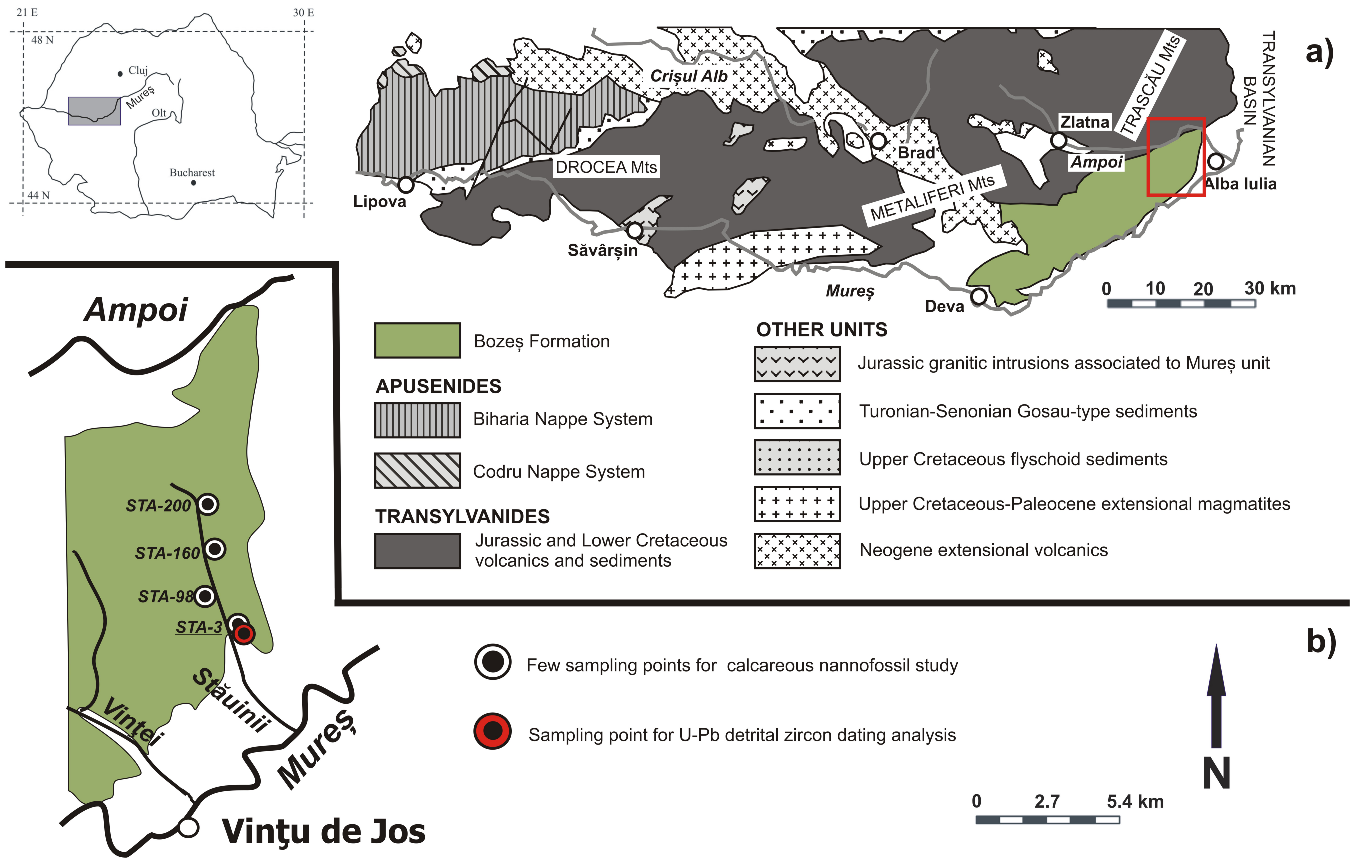

Fig. 1. *a) Sketch of the main tectonic units in the Southern Apuseni Mts, showing the location of the Bozeş Formation (simplified after Balintoni et al., 2009) and of the studied area (red square); b) Enlarged map of the western part of the Bozeş Formation, with location of Stăuinii valley and of some sampling points (modified after Lupu et al., 1967).*

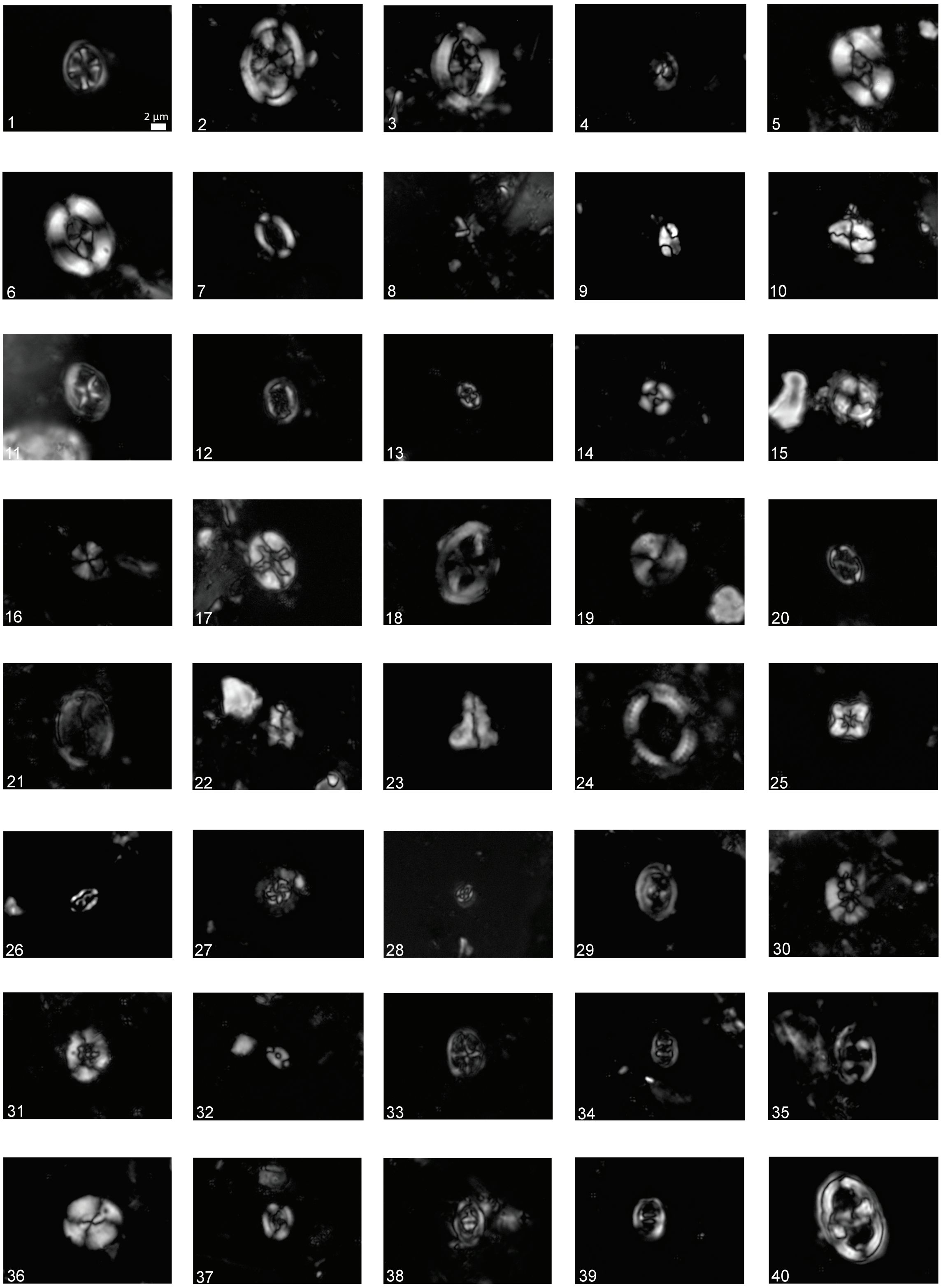

Fig. 2. *Calcareous nannofossils from Stauini Valley section. The photographs were taken under cross-polarized light.* **1)** Ahmuellerella octoradiata – *Samples 45;* **2)** Arkhangelskiella cymbiformis – *Sample 177;* **3)** Arkhangelskiella maastrichtiana – *Samples 168;* **4)** Biscutum constans – *Sample 167;* **5)** Broinsonia parca constricta – *Sample 172;* **6)** Broinsonia parca parca – *Sample 170;* **7)** Broinsonia parca expansa – *Sample 44;* **8)** Bukryaster hayi – *Sample 171;* **9)** Calculites obscurus – *Sample 25;* **10)** Calculites ovalis – *Sample 167;* **11)** Chiastozygus amphipons – *Sample 174;* **12)** Cribrosphaerella ehrenbergii – *Sample 45;* **13)** Corollithion madagaskariensis – *Sample 140;* **14)** Cyclagelosphaera rotaclypeata – *Sample 175;* **15)** Cylindralithus sculptus – *Sample 168;* **16)** Discorhabdus ignotus – *Sample 139;* **17)** Eiffelithus eximius – *Sample 176;* **18)** Gartnerago segmentatum – *Sample 139;* **19)** Haquis circumradiatus – *Sample 137;* **20)** Helicolithus trabeculatus – *Sample 143;* **21)** Kamptnerius magnificus – *Sample 139;* **22)** Lithastrinus grillii – *Sample 174;* **23)** Lucianorhabdus maleformis – *Sample 166;* **24)** Manivitella pemmatoidea – *Sample 132;* **25***)* Micula staurophora – *Sample 143;* **26)** Okkolithus australis – *Sample 26;* **27)** Prediscosphaera cretacea – *Sample 174;* **28)** Prediscosphaera stoveri – *Sample 44;* **29)** Reinhardtites anthophorus – *Sample 139;* **30)** Retecapsa angustiforata – *Sample 177;* **31)** Retecapsa crenulata – *Sample 45;* **32)** Russelia bukryi – *Sample 139;* **33)** Staurolithites imbricatus – *Sample 139;* **34)** Tranolithus minimus – *Sample 168;* **35)** Tranolithus orionatus – *Sample 166;* **36)** Watznaueria barnesiae – *Sample 167;* **37)** Watznaueria quadriradiata – *Sample 136;* **38)** Zeugrhabdotus bicrescenticus – *Sample 169;* **39)** Zeugrhabdotus diplogrammus – *Sample 168;* **40)** Zeugrhabdotus embergeri – *Sample 164*

are mentioned in Appendix 1. Relative abundance of each species and Shannon Index were calculated according to Murray (2006). For age determination biozonation schemes of Sissingh (1977), Perch-Nielsen (1985) and Burnett (1998) have been used.

Calcareous nannofossil assemblage results

The calcareous nannofossil assemblages contain 101 species. The preservation is poor to moderate. The diversity slightly increases toward the top of the section. A positive correlation between abundance and diversity can be recognized. The most abundant species is *Watznaueria barnesiae* (31.7–61.6%), followed by *Prediscosphaera cretacea* (3.4%–13%), *Micula staurophora* (0.6%-11%), *Retecapsa crenulata* (1.7%-11%), *Eiffelithus eximius* (0.7%-8.9%), *Tranolithus orionatus* (1.7%- 7%) and *Cribrosphaerella ehrenbergii* (1.4%-5.8%). Some important species are continuously present in the studied samples: *Broinsonia parca constricta, Broinsonia parca parca, Reinhardtites anthophorus, Lithastrinus grillii* together with rare specimens of *Lucianorhabdus cayeuxii.* The tethyan species are very rare: *Uniplanarius sissinghii* – 2 specimens; *Ceratolithoides aculeus* – 7 specimens and *Uniplanarius gothicus* – 6 specimens. Cold-water taxa are present in the assemblage, *Biscutum constans* being the most abundant (its abundance increases toward the top of the section, where it reaches 5%) together with *Ahmuellerella octoradiata, Gartnerago segmentatum, Zeugrhabdotus erectus, Prediscosphaera stoveri*, etc.

Age of sedimentary deposits

A detailed biozonation for the entire section is difficult to draw due to the bad preservation and absence of marker species. It is possible that the studied section begins with the Late Santonian due to the presence in some samples of curved *Lucianorhabdus cayeuxii*, a marker species for the uppermost Santonian – lowermost Campanian (Wagreich, 1992).

The presence in the analyzed samples of Campanian taxa such as *Broinsonia parca parca, Broinsonia parca constricta, Ceratolithoides aculeus, Uniplanarius sissinghii*, although some of them in a very low number, indicates a Campanian age of the deposits. Only three Campanian bioevents can be outlined: FO of *Reinhardites levis*, FO of *Prediscosphaera stoveri* and FO of *Eiffelithus parallelus*. The FO of *R. levis* is located in UC14 Zone (upper Lower Campanian) in the Tethyan Realm and in UC15 Zone (lower Upper Campanian) in the Boreal Realm (Burnett, 1998). *P. stoveri* is mentioned from both northern and southern hemispheres. In the North Sea its FO is placed at the base of $UC15_d^{BP}$ (lower Upper Campanian) (Burnett, 1998) and in *Biscutum coronum* Zone (upper Upper Campanian) in the Southern Hemisphere (Watkins et al., 1996). *E. parallelus* is used as a marker species for $UC15_d^{TP}$ – $UC15_e^{TP}$ (lower Upper Campanian to upper Upper Campanian), marking the top of $UC15_d^{TP}$ and the base of $UC15_e^{TP}$, respectively (Burnett, 1998).

In the studied deposits, *E. parallelus* has been identified in the samples collected from the upper part of the section, together with *E. eximius* and *R. anthophorus*. The last two mentioned species have their LO at the top of $UC15_e^{TP}$ (upper Upper Campanian). Thus, the upper part of the Stăuinii section falls in the $UC15_d^{TP}$ – $UC15_e^{TP}$ Subzones (Burnett, 1998), approximately equivalent to CC22 biozone (Sissingh, 1977; Perch-Nielsen, 1985). Therefore, the age of the top deposits of the Stăuinii Valley is Late Campanian, not reaching the Campanian/Maastrichtian boundary.

U-PB DETRITAL ZIRCON AGE ANALYSES

Due to its physical and chemical stability, detrital zircon is widespread in almost all siliciclastic rock types; therefore it is very useful in isotopic age investigation. The U-Pb dating of detrital zircon produces a spectrum of age populations, which can be used to constrain information on the age of the sediment sources, the orogenic history and paleogeography of ancient hinterlands, or even to establish the maximum depositional age of the sedimentary rock (*e.g.* Maas and McCulloch, 1991; Nelson, 2001; Avigad et al., 2003; Fedo et al., 2003).

Material and analytical methods

The sandstone selected for zircon U/Pb geochronological analysis (STA-3) was collected from the downvalley of the Stăuinii Stream (Fig. 1b). The sampling point is located in the uppermost part of the section, of Late Campanian age, as constrained by the calcareous nannofossil results, from above and below the sandstone level.

About 2 kg of fresh rock were crushed, sieved and treated with heavy liquid (diiodomethane) for separating the heavy mineral fraction. Zircon grains were hand-picked under a binocular microscope, all grain size and morphology being selected. The grains were mounted in epoxy and polished to expose their internal structure, which was revealed by cathodoluminiscence (CL) imaging using a Zeiss EVO50 SEM coupled to a CL detector system. U, Th, and Pb isotopes were measured for zircon grains by Laser Ablation with Inductively Coupled Plasma Mass Spectrometry (LA-ICP-MS) techniques using a Thermo-Scientific Element 2 XR sector field ICP-MS coupled to a New Wave UP-193 Excimer Laser System. The analysis used laser spot-sizes between 20 and 35 μm and consisted of 15s of background acquisition followed by 25s of data acquisition. A common-Pb correction based on the interference- and background-corrected 204Pb signal and a model Pb composition (Stacey and Kramers, 1975) was carried out if necessary. The raw data were corrected for background signal, common-Pb, laser induced elemental fractionation, instrumental mass discrimination and time- and depth dependant elemental fractionation of Pb/Th and Pb/U using an Excel® spreadsheet programme developed by Axel Gerdes (Institut für Geowissenschaften, Johann Wolfgang Goethe-Universität, Frankfurt am Main, Germany). For concordia diagrams (2 sigma error ellipses) and concordia ages (95% confidence level) Isoplot/Ex 2.49 (Ludwig, 2001) was used, while for frequency and relative probability plots AgeDisplay (Sircombe, 2004) was applied. More details on the analytical protocol and data processing can be found in Frei and Gerdes (2009).

Sample preparation was performed at the Babes-Bolyai University Cluj Napoca (Romania), Department of Geology, while CL images, LA-ICP-MS U–Pb analyses and age calculations were made at the Museum für Mineralogie und Geologie, Sektion Geochronologie, Senckenberg Naturhistorische Sammlungen Dresden (Germany).

U-Pb zircon dating results

Zircons extracted from the sample STA-3 are transparent, either rounded in shape or prismatic with variably rounded edges. 150 grains were ablated and 160 analyses were obtained. From the data set, 112 U-Pb ages are concordant between 90 and 110% and are considered for further discussions. Interpreted ages are based on $^{206}Pb/^{238}U$ for grains <1000 Ma and on $^{206}Pb/^{207}Pb$ for grains >1000 Ma in age.

The zircon age spectrum spans between 81 and 2650 Ma (Appendix 2). Nine grains give Archaen and Paleoproterozoic ages, and eight are Mesoproterozoic (Stenian, 1006-1152 Ma). The most consistent are the Neoproterozoic group with 48 ages (42%, 554-976 Ma) and the Paleozoic one, with 36 ages (32%, 432-536 Ma). Much younger are a Jurassic grain, of 164±3 Ma, and a population of Late Cretaceous age, represented by 10 $^{206}Pb/^{238}U$ ages between 81±2 and 91±2 Ma. The Paleozoic and older ages may be interpreted in terms of provenance, indicating ages of various sources which provided material for Bozeş rocks. Discussing the sources is beyond the purpose of this paper, and therefore these older ages will not be further considered.

U-Pb age of sedimentary deposition

Usually, the youngest detrital zircon age constrains the maximum age of deposition for a sedimentary rock. However, as a single analysis is statistically uncertain, a representative population of grains with analyses of good quality (high concordancy and analytical precision) should constrain the age of the youngest component (Kontinen et al., 2007). Crystallization ages of intruding or crosscutting magmatic rocks, if exist, or any other well-documented subsequent magmatic event will provide constraints on the minimum age of deposition (Nisbet, 1987).

From the 10 Late Cretaceous ages, the youngest 8 represent a consistent group with a concordia age of 82.87 ± 0.59 (MSWD=0.0014) (Fig. 3) and a maximum peak at 83 Ma on the probability density distribution (Fig. 4). Excluding from this group the two ages with the largest errors, the obtained concordia age, of 83.13 ± 0.64 (MSWD=0.0006) (Fig. 3), is slightly better constrained, but very similar with that of the whole youngest group. Thus, the maximum age of deposition for Bozeş sediments from Stăuinii Valley can be considered as around 83 Ma. However, the age of the youngest zircon in the group may be significant, and the maximum age of the deposition could be as young as 81±2 Ma. There are no data to precisely constrain the minimum age of sedimentary deposition for the studied deposits.

DISCUSSIONS

Calcareous nannofossils versus detrital zircons

The analysis of U-Pb detrital zircon ages indicates that the deposition of the sedimentary rocks on Stăuinii Valley started on around 83 Ma ago, thus in the Early Campanian, but there are no constraints on the duration of the sediment deposition. As

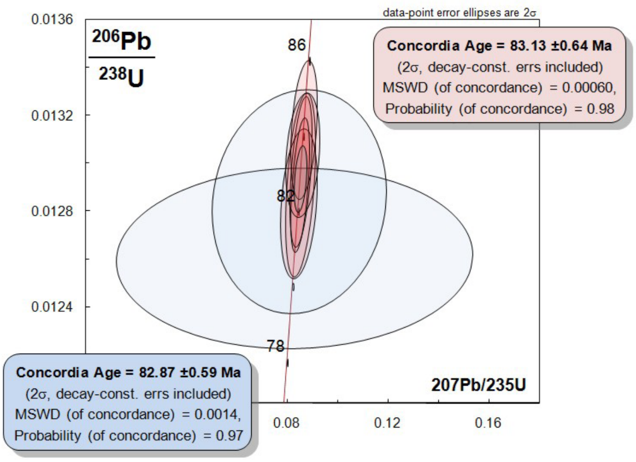

Fig. 3. *Concordia diagram and concordia ages for a group of 8 analyses of youngest zircons from sample STA-3 (concordia age in blue – of all group, in red – of group excluding two largest errors).*

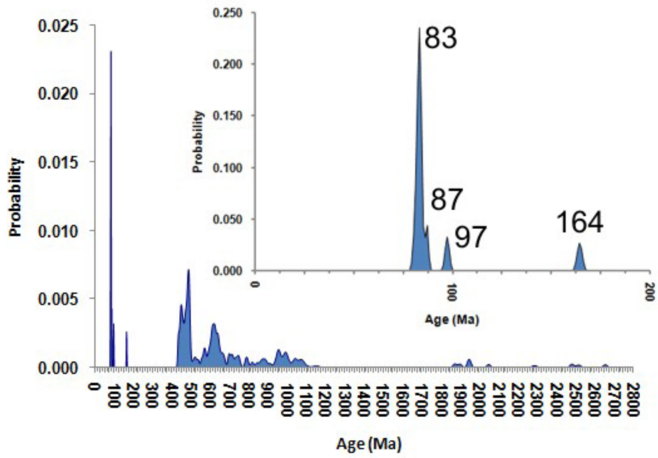

Fig. 4. *Probability density distribution plot of detrital zircon grains from sample STA-3. Inset shows enlarged interval of 0-200 Ma, with the corresponding ages of main peaks.*

revealed by the calcareous nannofossils investigation, the age of the studied deposits might start from Late Santonian and surely continues until the Late Campanian, below the boundary to the Maastrichtian. The detrital zircon age is more precise concerning the initiation of the sedimentation process, which is established at the lower limit of the Campanian, rather similar with the age of the calcareous nannofossils.

Each method has its own advantages and limitations. Due to the presence of a consistent young zircon population, U-Pb geochronology may date more precisely the initiation of sediment deposition, but fails in bracketing this process. On the other hand, calcareous nannofossil studies constrain an age interval for sediments, but the limits are sometimes questionable.

Presence or absence of Maastrichtian

Sediments of Early Maastrichtian age were mentioned on the Stăuinii Valley by Macovei and Atanasiu (1934), based on ammonite species *Pachydiscus neubergicus* and *P. colligatus*, described by Nopcsa (1905, in Macovei and Atanasiu, 1934). Among the recent studies performed on the sediments from Stăuinii Valley, Dimian and Popa-Dimian (1964) collected inoceramids from various stratigraphical levels, without finding *P. neubergicus*. The consistent foraminifera fauna mentioned by Dimian and Popa-Dimian (1964) also precludes the presence of the Early Maastrichtian in Stăuinii area. Few years later, *P. neubergicus* was reported by Tomescu et al. (1969) and used to advocate the presence of the Lower Maastrichtian deposits, although the authors mentioned it as part of a level with typical Late Campanian fauna. The calcareous nannofossil assemblages from Stăuinii Valley section, reported in the present study, argue for a Late Santonian (?) - Late Campanian age for the studied deposits, without any hint for a Maastrichtian age.

While *Pachydiscus colligatus* is described as a Late Campanian species (*e.g.* Főzy, 2001), *P. neubergicus* is usually considered a marker species for Early Maastrichtian, its FO being proposed as a biostratigraphic Campanian/Maastrichtian boundary criterion (*e.g.* Wagreich et al., 2003). *P. neubergicus* is now known in European occurrences from the Netherlands (Maastricht area), Denmark, northern Germany, France (Tercis), Spain, Austria (Neuberg), Bulgaria, etc. (Jagt & Felder, 2003). A correlation study of the local FO of *P. neubergicus* with calcareous nannofossil zone reveals that it has a rather long stratigraphical range, up to late Maastrichtian,

its local first occurrence being diachronous (Wagreich et al., 2003). Thus, although it is a Maastrichian fossil, it cannot be a reliable marker of the Campanian/Maastrichtian boundary, and additional dating methods are required (Wagreich et al., 2003).

However, it has been shown that the identification of *Pachydiscus* species is complicated, due to its morphology and to the existence of many names in the literature without precise description (Főzy, 2001). There are cases when the material originally determined as *P. neubergicus* was re-evaluated as different forms of *Pachydiscus*, *e.g. P. precolligatus*, *P. levyi* (Főzy, 2001) or *P. perfidus* (Machalski, 2012), which are Campanian in age.

In the Stăuinii Valley section, the presence of the Lower Maastrichtian deposits is inferred only from findings of *P. neubergicus*, as mentioned in two older studies (Nopcsa, 1905; Tomescu et al., 1969). Based on foraminifera (Dimian and Popa-Dimian, 1964) and calcareous nannofossil assemblages (this study), the upper age limit for the Stăuinii section is extended only to the Uppermost Campanian, and we regard the reported Maastrichtian as erroneous.

CONCLUSIONS

Several methods may be applied to establish the sedimentation age in case of siliciclastic rocks, including direct (fossils) and indirect (radiometric) techniques, each with advantages and limitations. The Stăuinii Valley deposits were the subject of several biostratigraphical studies, the results regarding their age being rather contradictory. Calcareous nannofossils and U-Pb detrital zircon were involved in order to compare and correlate the results. Both techniques yielded similar results, indicating probably an Early Campanian age (around 83 Ma) for the initiation of sediment deposition, but only calcareous nannofossil assemblage succeeded to constrain the ending of sedimentation, as Uppermost Campanian.

The presence of the Lower Maastrichtian deposits on the Stăuinii Valley is questioned as it is sustained only by old findings of *Pachydiscus neubergicus*. Based on other microfossil assemblages, as foraminifera or calcareous nannofossils, the upper age limit of the studied deposits is considered as Late Campanian, excluding the Lower Maastrichtian deposits from the Stăuinii section.

Acknowledgements. This study was financially supported by CNCSIS-UEFISCSU, project PN II-RU_TE_ 313/2010. Many thanks are due to Mandy Hofmann and Andreas Gartner (Senckenberg Naturhistorische Sammlungen Dresden (Germany) for their help during the zircon dating. We thank two anonymous reviewers for their corrections and suggestions, which helped us improve the manuscript.

REFERENCES

Avigad, D., Kolodner, K., McWilliams, M., Persing, H. & Weissbrod, T. 2003, Origin of northern Gondwana Cambrian sandstone revealed by detrital zircon SHRIMP dating. *Geology,* 31: 227-230. http://dx.doi.org/10.1130/0091-7613(2003)031<0227:OONGCS>2.0.CO;2

Balintoni, I. 1997, *Geotectonics of the metamorphic terrains from Romania*. Ed. Carpatica, 176 p (in Romanian).

Balintoni, I. 2003, Towards an improved model of the Laramian Transylvanides. *Studia UBB Geologia, Special Issue*: 13-20.

Balintoni, I., Balica, C., Cliveţi, M., Li, Q-L., Hann, H.P., Chen, F. & Schuller, V. 2009, The emplacement age of the Muntele Mare Variscan granite (Apuseni Mountains, Romania). *Geologica Carpathica*, 60 (6): 495-504. http://dx.doi.org/10.2478/v10096-009-0036-x

Bălc, R., Suciu-Krausz, E. & Borbei, F. 2007, Biostratigraphy of the Cretaceous deposits in the Western Transylvanides from Ampoi Valley (Southern Apuseni Mountains, Romania). *Studia UBB Geologia*, 52 (2): 37- 43. http://dx.doi.org/10.5038/1937-8602.52.2.5

Bălc, R., Silye, L. & Zaharia, L. 2012, Calcareous nannofossils and sedimentary facies in the Upper Cretaceous Bozeş Formation (Southern Apuseni Mountains, Romania). *Studia UBB Geologia*, 57 (1): 23-32. http://dx.doi.org/10.5038/1937-8602.57.1.3

Bleahu, M., Bordea, S., Lupu, M., Ştefan, A., Patrulius, D. & Panin, Ş. 1981, *The structure of the Apuseni Mountains*. Guide to Excursion B3, Carpatho-Balkan Geological Association XII Congress of Geology and Geophysics, 107 p.

Bown, P.R., Young, J.R. 1998, Techniques. In *Calcareous nannofossil stratigraphy* (Bown, P.R., Ed.): British Micropaleontology Society Series, Chapman & Hall, London, p. 16-28.

Bown, P.R., Rutledge, D.C., Crux, J.A. & Gallagher, L.T. 1998, Lower Cretaceous. In *Calcareous nannofossil stratigraphy* (Bown, P.R., Ed.): British Micropaleontology Society Series, Chapman & Hall, London, p. 86-131.

Burnett, J.A. 1998, Upper Cretaceous. In *Calcareous nannofossil stratigraphy* (Bown, P.R., Ed): British Micropaleontology Society Series, Chapman & Hall, London, p. 132-199.

Csontos, L. 1995, Tertiary tectonic evolution of the Intra-Carpathian area. *Acta Vulcanologica*, 7 (2): 1-13.

Dimian, E., Popa-Dimian, M. 1964, Stratigraphic and sedimentologic data on cretaceous formations between Mureş Valley and Ampoi Valley. *Dări de Seamă ale Institului de Geologie*, L (1): 107-103 (in Romanian).

Fedo, C.M., Sircombe, K.N. & Rainbird, R.H. 2003, Detrital zircon analysis of the sedimentary record. In *Zircon* (Hanchar, J., Hoskin, P.W.O, Eds.): *Reviews in Mineralogy and Geochemistry*, 53: 277-303.

Frei, D, Gerdes, A. 2009, Precise and accurate in situ U–Pb dating of zircon with high sample throughput by automated LA-SF-ICP-MS. *Chemical Geology*, 261: 261-270. http://dx.doi.org/10.1016/j.chemgeo.2008.07.025

Főzy, I. 2001, Campanian (Late Cretaceous) cephalopods from Sümeg (Transdanubian Central Range, Hungary). *Fragmenta Palaeontologica Hungarica,* 19: 25-37.

Ghiţulescu, T.P., Socolescu, M. 1941, Etude geologiques et miniere des Monts Metalliferes. *Anuarul Institutului Geologic,* XXI: 181- 463.

Ianovici, V., Borcoş, M., Bleahu, M., Patrulius, D., Lupu, M., Dimitrescu, R. & Savu, H. 1976, *Geology of Apuseni Mountains*. Ed. Academiei R.S.R., 631 p. (in Romanian).

Jagt, J.W.M., Felder, W.M. 2003, The stratigraphic range of the index ammonite *Pachydiscus neubergicus* (Hauer, 1858) in the type area of the Maastrichtian Stage. *Netherlands Journal of Geosciences / Geologie en Mijnbouw*, 82 (3): 261-268.

Kontinen, A., Käpyaho, A., Huhmab, H., Karhu, J., Matukov, D.I., Larionov, A. & Sergeev, S.A. 2007, Nurmes paragneisses in eastern Finland, Karelian craton: Provenance tectonic setting and implications for Neoarchaean craton correlation. *Precambrian Research*, 152: 119-148.
http://dx.doi.org/10.1016/j.precamres.2006.11.001

Ludwig, K.R. 2001, User's Manual for Isoplot/Ex rev. 2.49. *Berkeley Geochronology Center, Publication* 1a, 56 p.

Lupu, M., Borcos, M., Dimian, M., Lupu, D. & Dimitrescu, R. 1967, Geological map of Romania, scale 1:200.000, Turda sheet. Geological Institute of Romania.

Maas, R., McCulloch, M.T. 1991, The provenance of Archean clastic metasediments in the Narryer Gneiss Complex, Western Australia: Trace element geochemistry, Nd isotopes, and U-Pb ages for detrital zircons. *Geochemica et Cosmochimica Acta*, 55: 1915-1932.
http://dx.doi.org/10.1016/0016-7037(91)90033-2

Macovei, G., Atanasiu, I. 1934, L'evolution geologique de la Roumanie – Cretace. *Anuarul Institutului Geologic*, XVI: 63-280.

Machalski, M. 2012, Stratigraphically important ammonites from the Campanian–Maastrichtian boundary interval of the Middle Vistula River section, central Poland. *Acta Geologica Polonica*, 62 (1): 91-116.
http://dx.doi.org/10.2478/v10263-012-0004-0

Marincaş, V. 1973, The age of Bozeş Beds. *Studia UBB Geologia*, 1: 39-46 (in Romanian)

Marincaş, V., Mânecan, D. 1971, Contributions a la stratigraphie du cretace superieur dans la region de Geoagiu. *Sargetia*, VIII: 21-37

Martini, E. 1971, Standard Tertiary and Quaternary calcareous nannoplankton zonation. In *Proceedings of the II Planktonic Conference* (Farinacci, A., Ed.), Edizioni Tecnoscienza, Roma: 739-785.

Murray, J. 2006, *Ecology and applications of benthic foraminifera*. Cambridge University Press, 462 p.
http://dx.doi.org/10.1017/CBO9780511535529

Nelson, D.R. 2001, An assessment of the determination of depositional ages for Precambrian clastic sedimentary rocks by U-Pb dating of detrital zircon. *Sedimentary Geology*, 141-142: 37-60.
http://dx.doi.org/10.1016/S0037-0738(01)00067-7

Nisbet, E.G., 1987. *The young Earth: an Introduction to Archaean geology*. Allen and Unwin, London, 402 p.
http://dx.doi.org/10.1007/978-94-011-6489-4

Okada, H., Bukry, D. 1980, Supplementary modification and introduction of code numbers to the law-latitude coccolith biostratigraphic zonation. *Marine Micropaleontology*, 5: 321-325. http://dx.doi.org/10.1016/0377-8398(80)90016-X

Perch-Nielsen, K. 1985, Mesozoic calcareous nannofossils. In *Plankton stratigraphy* (Bolli, H.M., Saunders, J.B., Perch-Nielsen, K., Eds). Cambridge University Press, 329-426.

Rasmussen, B. 2005, Radiometric dating of sedimentary rocks: the application of diagenetic xenotime geochronology. *Earth Sciences Reviews*, 68: 197-243.
http://dx.doi.org/10.1016/j.earscirev.2004.05.004

Săndulescu, M. 1984, *Geotectonics of Romania*. Ed. Tehnica, 336 p (in Romanian).

Sircombe, K.N. 2004, AGEDISPLAY: an EXCEL workbook to evaluate and display univariate geochronological data using binned frequency histograms and probability density distributions. *Computer Geosciences*, 30: 21-31.
http://dx.doi.org/10.1016/j.cageo.2003.09.006

Sissingh, W. 1977, Biostratigraphy of Cretaceous calcareous nannoplankton. *Geologie en Mijnbouw*, Den Haag, 56: 37-56.

Stacey, J.S., Kramers, J.D. 1975, Approximation of terrestrial lead isotope evolution by a two-stage model. *Earth and Planetary Science Letters*, 26 (2): 207-221.
http://dx.doi.org/10.1016/0012-821X(75)90088-6

Tomescu, C., Panin, Ş., Georgescu, F., Mantea, G. & Antonescu, E. 1969, Contributions to the Neocretaceous stratigraphy of deposits from Southern Apuseni Mountains. *Studii şi Cercetări de Geologie, Geofizică, Geografie (Geologie)*, 14 (1): 239-252 (in Romanian).

Wagreich, M. 1992, Correlation of Late Cretaceous calcareous nannofossil zones with ammonite zones and planktonic Foraminifera: the Austrian Gosau sections. *Cretaceous Research,* 13: 505-516.

Wagreich, M., Küchler, T. & Summesberger, H. 2003, Correlation of calcareous nannofossil zones to the local first occurrence of *Pachydiscus neubergicus* (von Hauer, 1858) (Ammonoidea) in European Upper Cretaceous sections. *Netherlands Journal of Geosciences / Geologie en Mijnbouw*, 82 (3): 283-288.
http://dx.doi.org/10.1016/0195-6671(92)90014-H

Watkins, D.K., Wise Jr., S.W., Pospichal, J.J. & Crux, J. 1996, Upper Cretaceous calcareous nannofossil biostratigraphy and paleoceanography of the Southern Ocean, In *Microfossils and Oceanic Environments* (Moguilevsky, A., Whatley, R., Eds.) Aberystwyth Press, Aberystwyth, U. K., p. 355-381.

Appendix 1. Taxonomic index

A full list of all taxa identified in the Stăuinii Valley.

Acutturis scottus (Risatti, 1973) Wind and Wise *in* Wise and Wind, 1977
Ahmuellerella regularis (Górka, 1957) Reinhardt and Górka, 1967
Ahmuellerella octoradiata (Górka, 1957) Reinhardt, 1966
Amphizygus brooksii Bukry, 1969
Arkhangelksiella confusa Burnett, 1998b
Arkhangelskiella cymbiformis Vekshina, 1959
Arkhangelskiella maastrichtiana Burnett, 1998b
Biscutum constans (Górka, 1957) Black, 1959 *in* Black and Barnes, 1959
Biscutum dissimilis Wind and Wise *in* Wise and Wind, 1977
Biscutum magnum Wind and Wise *in* Wise and Wind, 1977
Braarudosphaera bigelowii (Gran and Braarud, 1935) Deflandre, 1947a
Broinsonia parca (Stradner, 1963) Bukry, 1969, ssp. *constricta* Hattner et al., 1980
Broinsonia parca (Stradner, 1963) Bukry, 1969, ssp. *expansa* Wise and Watkins in Wise, 1983
Broinsonia parca (Stradner, 1963), Bukry 1969, ssp. *parca*
Broinsonia signata (Noël, 1969) Noël, 1970
Bukryaster hayi (Bukry, 1969) Prins and Sissingh *in* Sissingh, 1977
Calculites sp. Prins and Sissingh *in* Sissingh , 1977
Calculites obscurus (Deflandre, 1959) Prins and Sissingh *in* Sissingh, 1977
Calculites ovalis (Stradner, 1963) Prins and Sissingh *in* Sissingh, 1977
Ceratolithoides aculeus (Stradner, 1961) Prins and Sissingh *in* Sissingh 1977
Chiastozygus sp. Gartner, 1968
Chiastozygus amphipons (Bramlette and Martini, 1964) Gartner, 1968
Chiastozygus bifarius Bukry, 1969
Chiastozygus litterarius (Górka, 1957) Manivit, 1971
Corollithion exiguum Stradner, 1961
Corollithion madagaskarensis Perch-Nielsen, 1973
Corollithion signum Stradner, 1963
Cretarhabdus striatus (Stradner, 1963) Black, 1973
Cribrocorona gallica (Stradner 1963) Perch-Nielsen 1973
Cribrosphaerella ehrenbergii (Arkhangelsky, 1912) Deflandre *in* Pivetteau, 1952
Cyclagelosphaera margerellii Noël, 1965
Cyclagelosphaera reinhardtii (Perch-Nielsen, 1968) Romein, 1977
Cyclagelosphaera rotaclypeata Bukry, 1969
Cylindralithus sp. Bramlette and Martini, 1964
Cylindralithus sculptus Bukry, 1969
Discorhabdus ignotus (Górka, 1957) Perch-Nielsen, 1968
Eiffelithus eximius (Stover, 1966) Perch-Nielsen, 1968
Eiffelithus gorkae Reinhardt, 1965
Eiffelithus parallelus Perch-Nielsen, 1973
Eiffelithus turriseiffelii (Deflandre *in* Deflandre and Fert, 1954) Reinhardt, 1965
Eprolithus floralis (Stradner, 1962) Stover, 1966
Eprolithus rarus Varol, 1992
Gartnerago segmentatum (Stover, 1966) Thierstein, 1974
Haquis circumradiatus (Stover, 1966) Roth, 1978
Helicolithus anceps (Górka, 1957) Noël, 1970
Helicolithus trabeculatus (Górka, 1957) Verbeek, 1977
Kamptnerius magnificus Deflandre, 1959
Lithastrinus grillii Stradner, 1962
Lithastrinus quadricuspis Farhan, 1987
Lithastrinus septenarius Forchheimer, 1972
Loxolithus armilla (Black *in* Black and Barnes 1959) Noël, 1965
Lucianorhabdus arcuatus Forchheimer, 1972
Lucianorhabdus cayeuxii Deflandre, 1959
Lucianorhabdus maleformis Reinhardt, 1966
Manivitella pemmatoidea (Deflandre *in* Manivit, 1965) Thierstein, 1971
Markalius inversus (Deflandre *in* Deflandre and Fert, 1954) Bramlette and Martini, 1964
Marthasterites furcatus (Deflandre *in* Deflandre and Fert, 1954) Deflandre, 1959
Marthasterites simplex (Bukry, 1969) Burnett, 1998b
Microrhabdulus belgicus Haye and Towe, 1963
Microrhabdulus decoratus Deflandre, 1959
Microrhabdulus undosus Perch-Nielsen, 1973
Micula concava (Stradner *in* Martini and Stradner, 1960) Verbeek, 1976b
Micula staurophora (Gardet, 1955) Stradner, 1963
Munarinus sp. Risatti, 1973
Munarinus lesliae Risatti, 1973
Octolithus multiplus (Perch-Nielsen, 1973) Romein, 1979
Okkolithus australis Wind and Wise *in* Wise and Wind, 1977
Orastrum campanensis (Cepek, 1970) Wind and Wise *in* Wise and Wind, 1977
Pervilithus varius Crux, 1981
Placozygus fibuliformis (Reinhardt, 1964) Hoffmann, 1970
Prediscosphaera arkhangelskyi (Reinhardt, 1965) Perch-Nielsen, 1984
Prediscosphaera cretacea (Arkhangelsky, 1912) Gartner, 1968
Prediscosphaera grandis Perch-Nielsen, 1979a
Prediscosphaera ponticula (Bukry, 1969) Perch-Nielsen, 1984
Prediscosphaera spinosa (Bramlette and Martini, 1964) Gartner, 1968
Prediscosphaera stoveri (Perch-Nielsen, 1968) Shafik and Stradner, 1971
Quadrum gartneri Prins and Perch-Nielsen *in* Manivit el al., 1977
Reinhardtites anthophorus (Deflandre, 1959) Perch-Nielsen, 1968
Reinhardtites levis Prins and Sissingh *in* Sissingh, 1977
Retecapsa angustiforata Black, 1971a
Retecapsa crenulata (Bramlette and Martini, 1964) Grün *in* Grün and Allemann, 1975
Rhagodiscus achlyostaurion (Hill, 1976) Doeven, 1983
Rhagodiscus angustus (Stradner, 1963) Reinhardt, 1971
Rhagodiscus reniformis Perch-Nielsen, 1973
Rhagodiscus splendens (Deflandre, 1953) Verbeek, 1977
Russelia bukryi Risatti, 1973

Russellia laswellii Risatti, 1973
Staurolithites sp. Caratini, 1963
Staurolithites ellipticus (Gartner, 1968) Lambert, 1987
Seribiscutum gaultensis Mutterlose, 1992a
Staurolithites imbricatus (Gartner, 1968) Burnett, 1998b
Staurolithites laffittei Caratini, 1963
Tranolithus minimus (Bukry, 1969) Perch-Nielsen, 1984
Tranolithus orionatus (Reinhardt, 1966a) Reinhardt, 1966b
Uniplanarius gothicus (Deflandre, 1959) Hattner and Wise, 1980
Uniplanarius sissinghii Perch-Nielsen, 1986b
Watznaueria barnesiae (Black, 1959) Perch-Nielsen, 1968
Watznaueria fossacincta (Black, 1971a) Bown *in* Bown and Cooper, 1989a
Watzanuaeria quadriradiata Bukry, 1969
Watznaueria ovata Bukry, 1969
Zeugrhabdotus sp. Reinhardt, 1965
Zeugrhabdotus bicrescenticus (Stover, 1966) Burnett *in* Gale et al., 1996
Zeugrhabdotus biperforatus
Zeugrhabdotus diplogrammus (Deflandre in Deflandre and Fert, 1954) Burnett *in* Gale et al., 1996
Zeugrhabdotus embergeri (Noël, 1958) Perch-Nielsen, 1984
Zeugrhabdotus erectus (Deflandre *in* Deflandre and Fert, 1954) Reinhardt, 1965
Zeugrhabdotus noeliae Rood et al., 1971
Zeugrhabdotus scutula (Bergen, 1994) Rutledge and Bown, 1996

Appendix 2. LA-ICPMS U-Pb Detrital zircon age data

U-Pb-Th data of zircon from sample STA-3, n = 112 of 160 measured zircon grains (90-110 % conc.), Late Cretaceous sandstone, Stăuinii Valley, Bozeș Formation, Romania.

Name (spot)	TH[a]/U	$^{206}Pb^b/^{238}U$	2σ (%)	$^{207}Pb^b/^{235}U$	2σ (%)	$^{207}Pb^b/^{206}Pb$	2σ (%)	Rho[c]	$^{206}Pb/^{238}U$	±2 σ (Ma)	$^{207}Pb/^{235}U$	±2 σ (Ma)	$^{207}Pb/^{206}Pb$	±2 σ (Ma)	Conc (%)
STA 3-seq1-a52	**0.71**	0.01261	2.4	0.0828	69.8	0.0476	69.8	0.04	**81**	**2**	81	56	81	1657	100
STA 3-seq1-a48	**0.25**	0.01284	2.0	0.0843	7.1	0.0476	6.8	0.28	**82**	**2**	82	6	81	162	101
STA 3-seq1-a49	**0.27**	0.01285	3.0	0.0845	33.4	0.0477	33.3	0.09	**82**	**2**	82	27	85	789	97
STA 3-seq2-B56	**0.49**	0.01291	1.8	0.0849	3.4	0.0477	2.9	0.52	**83**	**1**	83	3	83	70	100
STA 3-seq3-C54	**0.30**	0.01291	2.4	0.0849	5.8	0.0477	5.3	0.42	**83**	**2**	83	5	84	126	98
STA 3-seq2-B02	**0.24**	0.01297	2.0	0.0852	4.2	0.0477	3.7	0.47	**83**	**2**	83	3	83	88	100
STA 3-seq2-B55	**0.42**	0.01304	1.6	0.0859	6.5	0.0478	6.3	0.25	**84**	**1**	84	5	87	150	96
STA 3-seq2-B04	**0.26**	0.01314	1.8	0.0865	5.1	0.0477	4.7	0.36	**84**	**2**	84	4	85	112	99
STA 3-seq2-B19	**0.74**	0.01355	1.8	0.0893	6.4	0.0478	6.2	0.28	**87**	**2**	87	5	89	146	97
STA 3-seq2-B18	**0.42**	0.01517	2.3	0.1004	6.4	0.0480	6.0	0.35	**97**	**2**	97	6	99	143	98
STA 3-seq2-B52	**0.45**	0.02579	1.6	0.1754	3.9	0.0493	3.5	0.42	**164**	**3**	164	6	164	82	100
STA 3-seq2-B25	**0.26**	0.06937	1.5	0.5403	1.8	0.0565	1.0	0.82	**432**	**6**	439	7	472	23	92
STA 3-seq1-a27	**0.40**	0.07011	2.0	0.5371	2.5	0.0556	1.4	0.83	**437**	**9**	437	9	435	30	100
STA 3-seq1-a38	**0.06**	0.07043	2.4	0.5400	3.1	0.0556	1.9	0.78	**439**	**10**	438	11	437	43	101
STA 3-seq3-C32	**0.09**	0.07059	3.4	0.5434	4.1	0.0558	2.3	0.83	**440**	**14**	441	15	446	51	99
STA 3-seq1-a44	**0.44**	0.07127	2.0	0.5474	2.4	0.0557	1.4	0.82	**444**	**8**	443	9	441	31	101
STA 3-seq1-a30	**0.06**	0.07180	2.1	0.5561	3.1	0.0562	2.3	0.68	**447**	**9**	449	11	459	50	97
STA 3-seq2-B30	**0.29**	0.07182	1.9	0.5560	3.2	0.0561	2.5	0.61	**447**	**8**	449	12	458	56	98
STA 3-seq3-C16	**0.32**	0.07233	2.4	0.5591	2.7	0.0561	1.2	0.89	**450**	**11**	451	10	455	28	99
STA 3-seq1-a25	**0.21**	0.07247	2.2	0.5586	3.4	0.0559	2.5	0.66	**451**	**10**	451	12	448	56	101
STA 3-seq1-a26	**0.50**	0.07252	2.3	0.5581	2.7	0.0558	1.4	0.86	**451**	**10**	450	10	445	31	101
STA 3-seq3-C26	**0.10**	0.07354	2.4	0.5694	3.1	0.0562	2.0	0.76	**457**	**10**	458	11	459	44	100
STA 3-seq3-C46	**0.08**	0.07367	2.3	0.5695	2.9	0.0561	1.7	0.80	**458**	**10**	458	11	455	38	101
STA 3-seq3-C17	**0.11**	0.07436	2.6	0.5756	3.6	0.0561	2.5	0.72	**462**	**12**	462	14	458	55	101
STA 3-seq1-a60	**0.11**	0.07451	3.2	0.5877	4.9	0.0572	3.7	0.65	**463**	**14**	469	19	499	82	93
STA 3-seq3-C60	**0.27**	0.07478	3.2	0.5864	3.6	0.0569	1.7	0.88	**465**	**14**	469	14	486	38	96
STA 3-seq2-B12	**0.21**	0.07553	2.0	0.5890	3.1	0.0566	2.3	0.66	**469**	**9**	470	12	475	51	99
STA 3-seq3-C47	**0.09**	0.07589	2.4	0.5926	3.3	0.0566	2.2	0.73	**472**	**11**	473	12	477	49	99
STA 3-seq3-C52	**0.34**	0.07594	2.2	0.5934	3.1	0.0567	2.1	0.73	**472**	**10**	473	12	479	47	99
STA 3-seq1-a57	**0.40**	0.07609	2.2	0.5962	3.4	0.0568	2.6	0.64	**473**	**10**	475	13	485	57	98
STA 3-seq2-B44	**0.12**	0.07715	1.7	0.6107	2.7	0.0574	2.1	0.63	**479**	**8**	484	11	507	47	94
STA 3-seq2-B21	**0.11**	0.07733	1.9	0.6185	3.6	0.0580	3.1	0.52	**480**	**9**	489	14	530	67	91
STA 3-seq1-a18	**0.08**	0.07737	2.7	0.6023	3.5	0.0565	2.2	0.77	**480**	**12**	479	13	470	49	102
STA 3-seq3-C02	**0.05**	0.07740	2.7	0.6081	3.9	0.0570	2.7	0.71	**481**	**13**	482	15	491	60	98
STA 3-seq3-C03	**0.14**	0.07815	2.5	0.6156	3.2	0.0571	2.1	0.77	**485**	**12**	487	13	497	45	98
STA 3-seq2-B40	**0.12**	0.07817	2.4	0.6096	2.9	0.0566	1.7	0.81	**485**	**11**	483	11	474	38	102
STA 3-seq2-B36	**0.06**	0.07818	2.1	0.6143	3.3	0.0570	2.6	0.63	**485**	**10**	486	13	491	57	99
STA 3-seq2-B26	**0.26**	0.07826	1.6	0.6135	2.6	0.0569	2.1	0.61	**486**	**7**	486	10	486	46	100
STA 3-seq2-B47	**0.15**	0.07840	2.2	0.6158	3.5	0.0570	2.7	0.63	**487**	**10**	487	14	490	60	99
STA 3-seq1-a08	**0.18**	0.07869	2.4	0.6263	2.9	0.0577	1.6	0.83	**488**	**11**	494	12	519	36	94
STA 3-seq1-a24	**0.11**	0.07890	2.1	0.6206	3.1	0.0570	2.3	0.68	**490**	**10**	490	12	493	50	99
STA 3-seq2-B38	**0.09**	0.07905	1.9	0.6219	3.0	0.0571	2.3	0.63	**490**	**9**	491	12	494	51	99
STA 3-seq1-a35	**0.44**	0.07912	1.9	0.6302	3.4	0.0578	2.9	0.55	**491**	**9**	496	13	521	63	94
STA 3-seq2-B22	**0.15**	0.07987	2.6	0.6306	3.6	0.0573	2.4	0.73	**495**	**12**	496	14	502	53	99
STA 3-seq3-C34	**0.26**	0.08265	2.7	0.6573	3.6	0.0577	2.3	0.76	**512**	**13**	513	14	518	51	99
STA 3-seq3-C37	**0.27**	0.08441	2.3	0.6829	2.9	0.0587	1.8	0.79	**522**	**11**	529	12	555	38	94
STA 3-seq1-a33	**0.64**	0.08669	2.2	0.6948	3.2	0.0581	2.3	0.70	**536**	**12**	536	14	535	51	100
STA 3-seq1-a21	**0.28**	0.08975	2.2	0.7464	2.7	0.0603	1.7	0.79	**554**	**11**	566	12	615	36	90
STA 3-seq3-C48	**0.54**	0.09207	2.2	0.7607	2.6	0.0599	1.4	0.84	**568**	**12**	574	12	601	31	95
STA 3-seq3-C06	**0.23**	0.09259	2.9	0.7557	3.5	0.0592	1.9	0.84	**571**	**16**	572	15	574	42	99
STA 3-seq1-a23	**0.52**	0.09278	2.6	0.7630	3.2	0.0596	1.8	0.82	**572**	**14**	576	14	591	39	97
STA 3-seq3-C14	**0.26**	0.09566	2.5	0.8064	3.0	0.0611	1.6	0.84	**589**	**14**	600	13	644	34	91

Name (spot)	TH^a/U	$^{206}Pb^b/^{238}U$	2σ (%)	$^{207}Pb^b/^{235}U$	2σ (%)	$^{207}Pb^b/^{206}Pb$	2σ (%)	Rho[c]	$^{206}Pb/^{238}U$	±2 σ (Ma)	$^{207}Pb/^{235}U$	±2 σ (Ma)	$^{207}Pb/^{206}Pb$	±2 σ (Ma)	Conc (%)
STA 3-seq3-C15	0.20	0.09617	2.3	0.8010	2.9	0.0604	1.9	0.77	592	13	597	13	618	40	96
STA 3-seq2-B54	0.75	0.09744	2.1	0.8059	3.0	0.0600	2.2	0.68	599	12	600	14	603	48	99
STA 3-seq2-B32	0.36	0.09833	2.0	0.8281	2.6	0.0611	1.7	0.75	605	11	613	12	642	37	94
STA 3-seq2-B23	0.20	0.09885	2.3	0.8191	2.9	0.0601	1.8	0.78	608	13	608	13	607	40	100
STA 3-seq1-a06	0.40	0.09945	1.7	0.8339	2.2	0.0608	1.4	0.77	611	10	616	10	633	31	97
STA 3-seq3-C44	0.97	0.09975	2.5	0.8377	3.2	0.0609	2.0	0.79	613	15	618	15	636	43	96
STA 3-seq1-a37	0.81	0.10006	2.1	0.8440	2.8	0.0612	1.8	0.76	615	12	621	13	645	39	95
STA 3-seq3-C07	0.36	0.10033	2.7	0.8390	3.0	0.0606	1.3	0.89	616	16	619	14	627	29	98
STA 3-seq2-B42	0.89	0.10099	1.7	0.8316	2.7	0.0597	2.2	0.61	620	10	614	13	594	47	104
STA 3-seq2-B60	0.46	0.10163	1.8	0.8479	2.6	0.0605	1.9	0.68	624	11	624	12	622	42	100
STA 3-seq1-a56	0.70	0.10163	2.1	0.8412	2.9	0.0600	2.0	0.74	624	13	620	14	605	43	103
STA 3-seq1-a20	0.53	0.10253	1.7	0.8589	2.1	0.0608	1.3	0.79	629	10	630	10	631	28	100
STA 3-seq3-C13	0.20	0.10363	2.3	0.8765	2.9	0.0613	1.7	0.80	636	14	639	14	651	37	98
STA 3-seq2-B41	0.64	0.10383	1.9	0.8632	2.7	0.0603	2.0	0.69	637	11	632	13	614	43	104
STA 3-seq2-B27	1.12	0.10428	1.9	0.8841	2.6	0.0615	1.9	0.70	639	11	643	13	657	40	97
STA 3-seq2-B28	2.17	0.10453	2.0	0.8777	3.6	0.0609	3.0	0.56	641	12	640	17	636	65	101
STA 3-seq1-a01	0.40	0.10598	1.8	0.8957	2.6	0.0613	1.9	0.69	649	11	649	12	650	40	100
STA 3-seq2-B34	0.34	0.10790	2.2	0.9128	2.8	0.0614	1.7	0.79	661	14	659	14	652	37	101
STA 3-seq3-C08	0.43	0.10807	2.5	0.9134	3.1	0.0613	1.8	0.81	662	16	659	15	650	39	102
STA 3-seq1-a36	0.09	0.11000	2.2	0.9334	2.9	0.0615	1.9	0.76	673	14	669	14	658	40	102
STA 3-seq2-B13	0.31	0.11400	1.7	0.9791	2.7	0.0623	2.1	0.61	696	11	693	14	684	46	102
STA 3-seq3-C51	0.19	0.11463	2.7	1.0199	3.4	0.0645	2.0	0.81	700	18	714	17	759	42	92
STA 3-seq1-a45	0.25	0.11682	1.9	1.0084	3.4	0.0626	2.8	0.56	712	13	708	17	695	60	102
STA 3-seq3-C35	0.46	0.11777	2.8	1.0194	4.9	0.0628	4.0	0.57	718	19	714	25	701	85	102
STA 3-seq2-B50	0.13	0.12017	1.9	1.0810	2.7	0.0652	2.0	0.68	732	13	744	15	782	42	94
STA 3-seq1-a15	0.38	0.12232	1.8	1.1001	4.4	0.0652	4.0	0.42	744	13	753	24	782	83	95
STA 3-seq1-a17	1.76	0.12344	2.4	1.1097	4.2	0.0652	3.4	0.57	750	17	758	23	781	72	96
STA 3-seq3-C29	0.30	0.12976	2.3	1.1676	3.1	0.0653	2.1	0.75	787	17	786	17	783	43	100
STA 3-seq3-C41	0.36	0.13017	2.3	1.1778	4.0	0.0656	3.2	0.57	789	17	790	22	794	68	99
STA 3-seq1-a46	0.41	0.13506	2.1	1.2543	2.6	0.0674	1.6	0.79	817	16	825	15	849	34	96
STA 3-seq3-C09	0.52	0.13949	2.3	1.3133	5.0	0.0683	4.4	0.47	842	18	852	29	877	91	96
STA 3-seq3-C24	0.43	0.14348	2.3	1.3361	3.5	0.0675	2.7	0.64	864	18	862	21	854	56	101
STA 3-seq3-C40	0.56	0.14536	2.8	1.3569	3.2	0.0677	1.6	0.87	875	23	871	19	859	32	102
STA 3-seq3-C59	0.49	0.14728	2.1	1.3817	2.7	0.0680	1.6	0.79	886	18	881	16	870	33	102
STA 3-seq1-a51	0.06	0.15141	2.5	1.4448	2.8	0.0692	1.3	0.89	909	21	908	17	905	26	100
STA 3-seq3-C43	0.42	0.15671	2.3	1.5479	2.8	0.0716	1.7	0.80	938	20	950	18	976	34	96
STA 3-seq2-B11	0.52	0.15925	1.9	1.5791	2.8	0.0719	2.1	0.68	953	17	962	18	984	42	97
STA 3-seq1-a31	0.39	0.15939	2.4	1.5873	3.4	0.0722	2.4	0.70	953	21	965	21	992	49	96
STA 3-seq3-C22	0.52	0.16009	2.2	1.6184	2.5	0.0733	1.2	0.88	957	19	977	16	1023	24	94
STA 3-seq3-C39	0.56	0.16391	2.6	1.6407	3.2	0.0726	1.8	0.82	978	24	986	20	1003	37	98
STA 3-seq2-B08	0.64	0.16582	2.1	1.6571	2.7	0.0725	1.7	0.78	989	19	992	17	999	34	99
STA 3-seq1-a10	0.29	0.16716	2.4	1.6869	2.8	0.0732	1.5	0.84	996	22	1004	18	1019	31	98
STA 3-seq3-C55	0.74	0.17080	2.1	1.6870	3.0	0.0716	2.1	0.72	1017	20	1004	19	976	43	104
STA 3-seq1-a58	0.28	0.17441	2.5	1.7485	4.3	0.0727	3.4	0.59	1036	24	1027	28	1006	70	103
STA 3-seq1-a19	0.61	0.17153	1.9	1.7197	2.6	0.0727	1.9	0.71	1021	18	1016	17	1006	38	101
STA 3-seq1-a16	0.19	0.17560	1.8	1.7892	2.0	0.0739	0.9	0.88	1043	17	1042	13	1039	19	100
STA 3-seq2-B43	0.99	0.17707	3.0	1.8139	3.5	0.0743	1.9	0.84	1051	29	1050	23	1049	38	100
STA 3-seq1-a05	0.74	0.17152	2.7	1.7752	3.4	0.0751	2.1	0.79	1021	26	1036	23	1070	42	95
STA 3-seq3-C31	0.32	0.18175	2.4	1.8845	2.7	0.0752	1.3	0.88	1077	24	1076	18	1074	26	100
STA 3-seq2-B06	0.57	0.18362	2.0	1.9183	3.3	0.0758	2.7	0.59	1087	20	1087	23	1089	54	100
STA 3-seq1-a07	0.34	0.18812	2.6	2.0289	3.3	0.0782	2.1	0.77	1111	26	1125	23	1152	42	96
STA 3-seq3-C19	0.38	0.34109	2.2	5.3726	2.5	0.1142	1.2	0.87	1892	37	1881	22	1868	22	101
STA 3-seq1-a13	0.33	0.33732	1.9	5.3996	2.3	0.1161	1.3	0.82	1874	30	1885	20	1897	23	99
STA 3-seq2-B20	0.38	0.34240	2.1	5.6212	2.4	0.1191	1.0	0.91	1898	35	1919	21	1942	17	98
STA 3-seq1-a29	0.62	0.34357	2.4	5.6530	2.8	0.1193	1.5	0.85	1904	40	1924	25	1946	26	98
STA 3-seq3-C01	0.26	0.36577	2.5	6.3621	2.9	0.1262	1.4	0.88	2009	44	2027	26	2045	25	98

Name (spot)	TH[a]/U	$^{206}Pb^b/^{238}U$	2σ (%)	$^{207}Pb^b/^{235}U$	2σ (%)	$^{207}Pb^b/^{206}Pb$	2σ (%)	Rho[c]	$^{206}Pb/^{238}U$	±2 σ (Ma)	$^{207}Pb/^{235}U$	±2 σ (Ma)	$^{207}Pb/^{206}Pb$	±2 σ (Ma)	Conc (%)
STA 3-seq2-B53	**.067**	0.41207	2.1	8.2172	2.9	0.1446	2.0	0.72	**2224**	**39**	2255	26	2283	35	**97**
STA 3-seq3-C11	**0.17**	0.48162	2.7	10.7532	3.0	0.1619	1.4	0.89	**2534**	**57**	2502	29	2476	23	**102**
STA 3-seq2-B03	**0.73**	0.47820	1.7	10.9146	2.4	0.1655	1.7	0.71	**2519**	**37**	2516	23	2513	29	**100**
STA 3-seq3-C25	**1.06**	0.52094	2.3	12.9103	2.8	0.1797	1.6	0.83	**2703**	**51**	2673	27	2650	26	**102**

[a]U and Pb content and Th/U ratio were calculated relative to GJ-1 and are accurate to approximately 10%.
[b]corrected for background, mass bias, laser induced U-Pb fractionation and common Pb (if detectable, see analytical method) using Stacey & Kramers (1975)
[c]Rho is the error correlation defined as err206Pb/238U/err207Pb/235U.